Lawrence Berkeley Laboratory
UNIVERSITY OF CALIFORNIA

Materials & Chemical Sciences Division

Incommensurable Surface Spin Structures in MnO-type Antiferromagnets

DO NOT MICROFILM
COVER

L.M. Falicov and D.C. Chrzan

May 1989

MASTER

DISCLAIMER

DISCLAIMER

Incommensurable Surface Spin Structures in MnO-type Antiferromagnets

L. M. Falicov

and

D. C. Chrzan

Department of Physics,
University of California,
Berkeley, CA 94720,

and

Materials and Chemical Sciences Division,
Lawrence Berkeley Laboratory,
Berkeley, CA 94720.

ABSTRACT

A theory for the phase stability of incommensurable spin structures on the {001} surfaces of the rock-salt antiferromagnets is presented. It consists of classical spins and a simple Heisenberg Hamiltonian dependent on three exchange interactions: (a) a surface-only nearest-neighbor exchange; (b) a surface-second-layer nearest-neighbor exchange; and (c) an antiferromagnetic second-nearest-neighbor superexchange throughout the crystal. Incommensurable magnetic surface structures are proven to be the ground state for a wide range of the surface exchange parameters.

DISCLAIMER

May 11, 1989

Incommensurable Surface Spin Structures in MnO-type Antiferromagnets

L. M. Falicov

and

D. C. Chrzan

Department of Physics,
University of California,
Berkeley, CA 94720,

and

Materials and Chemical Sciences Division,
Lawrence Berkeley Laboratory,
Berkeley, CA 94720.

I. Introduction

The Europium monochalcogenides are magnetic semiconductors.[1] They display a variety of magnetic behaviors: EuO and EuS are ferromagnets, EuTe is an antiferromagnet, and EuSe is ferromagnetic below 2.8 K, and antiferromagnetic[2] between 2.8 K and 4.6 K.

The magnetism in these compounds arises primarily from exchange interactions involving the localized $4f$-shell electrons of the Eu atoms.[1] In the rock-salt structure of EuX, where X is O, S, Se, or Te, the Eu atoms are located on a face-centered-cubic lattice. The varied magnetic structures observed in the EuX compounds are a consequence of the competition between dipole-dipole interactions[3] and three exchange processes: (i) the direct overlap of the hybridized Eu $4f - 5d$ orbitals with the twelve neighboring Eu orbitals (generally ferromagnetic); (ii) the superexchange[4] interaction through the valence band formed largely from the p orbitals of X (antiferromagnetic); and (iii) a nearest-neighbor indirect exchange[5] through the conduction band (either antiferromagnetic or ferromagnetic depending on the amount of doping). Because of

the axial nature of the p orbitals of X, the superexchange mechanism is strongly directed and vanishes for nearest-neighbor Eu atoms.[6] The resulting stable magnetic structures[7] consist of (111) ferromagnetically aligned planes, with alternate planes aligned either parallel (ferromagnets), or antiparallel (antiferromagnets) to each other. The antiferromagnetic structure has been observed[6] in the transition-metal oxides (NiO, CoO, MnO, and FeO), and in EuTe.

The surfaces of these compounds display anomalous magnetic properties.[8,9] Techniques which probe the surface magnetic structure either directly (e.g. low-energy electron diffraction (LEED),[8,10–12] spin-polarized low-energy electron diffraction (SPLEED),[8] or indirectly, (e.g. spin-polarized photoemission[13–18]) have provided valuable experimental results. In the experiment which prompted this research,[19] Grazhulis and collaborators report the appearance of symmetry-breaking incommensurable surface spin-structures with temperature dependent wavevectors in low temperature ($\approx$ 10 K) LEED studies of single-crystal EuTe {001} surfaces obtained by cleavage under ultrahigh vacuum conditions.

The calculation presented here[20,21] demonstrates that the stability of the incommensurable magnetic structures on the {001} surfaces of EuTe, observed by Grazhulis and coworkers, most likely originates in the competition between relatively large surface nearest-neighbor exchanges and the second-nearest-neighbor superexchange interactions characteristic of the bulk. The calculation, based on a classical Heisenberg Hamiltonian at zero temperature, includes all possible commensurable structures plus one class of incommensurable surface spin arrangements; it yields a complex phase-stability diagram (as a function of surface exchange integrals) with regions of commensurable and incommensurable ground-state-structures.

II. Calculations

Three exchange integrals enter the calculation: J, the superexchange between second-nearest neighbors throughout the crystal; K, the net exchange between nearest neighbors on the surface; and L, the net exchange between nearest neighbors where one atom is in the surface layer, and the other is in the second layer. Because only the antiferromagnets are considered, J is restricted to be positive, but K and L are allowed to have either sign. Nearest-neighbor exchange in the bulk is neglected and all layers, except the two surface layers, are assumed to have the bulk antiferromagnetic configuration.

The total energy is written

$$E = J \sum_{(ij)} S_i \cdot S_j + K \sum_{<ij>} S_i \cdot S_j + L \sum_{[ij]} S_i \cdot S_j \qquad , \qquad (1)$$

where S_i is a classical spin of unit magnitude fixed at site i, (ij) designates a second-nearest-neighbor pair, $<ij>$ is a nearest-neighbor pair with both spins at the surface, and $[ij]$ is a nearest-neighbor pair with one spin at the surface and one in the second layer; the sums run over an infinite half space.

The two-dimensional unit cell chosen for the calculation contains four atoms from each plane. The cell, with linear dimension b, and its Brillouin zone are shown in figure 1. (The spins are depicted in the chosen bulk configuration.) The points Y and Y' in the Brillouin zone are not equivalent because the spin domain structure of the bulk introduces a preferred direction on the surface.

The Eu face-centered-cubic lattice is divided into four interpenetrating simple-cubic lattices each of which is further divided into two interpenetrating face-centered-cubic lattices. Each simple-cubic sublattice is denoted by a subscript i which runs from A to D. Each face-centered-cubic sub-sublattice corresponding to a given simple-cubic sublattice is designated by the subscript μ, which is either α or β.

The trial spin configurations in the two topmost layers have the form of a "frozen", finite-amplitude spin-wave:

$$S_{i\mu}(R) = x_{i\mu} \cos (k \cdot R + \phi_{i\mu}) \; \hat{x} + y_{i\mu} \sin (k \cdot R + \phi_{i\mu}) \; \hat{y} + z_{i\mu} \; \hat{z} \quad , \qquad (2)$$

$$x_{i\mu}^2 = y_{i\mu}^2 = 1 - z_{i\mu}^2 \quad ,$$

where $\hat{z}$ in a unit vector in the direction of the bulk spin quantization, R refers to the position of the unit cell, and k lies in the Brillouin zone of figure 2. States with $k = 0$ are referred to as commensurable, and states with $k \neq 0$ are called incommensurable. The spins of (2) have magnitude unity and the energy given by (1)-(2) is easily summed to obtain a closed expression for the energy per unit cell for all k, including those at the zone edge.

All spins not in the top two layers are kept fixed:

$$x_{i\mu} = y_{i\mu} = 0 \quad , \qquad (3a)$$

and

$$z_{i\alpha} = 1 , \qquad z_{i\beta} = -1 \quad . \qquad (3b)$$

The total energy (1)-(2), for given values of (K/J) and (L/J) in the range $-5 \leq (K/J) \leq 5$ and $-5 \leq (L/J) \leq 5$, is minimized with respect to $x_{i\mu}$, $y_{i\mu}$, k, and $\phi_{i\mu}$.

III. Results and Discussion

The minimum-energy phase-stability diagram is shown in figure 2. It contains commensurable [$k = 0$ in (2), unshaded regions in the figure] as well as incommensurable spin structures [$k \neq 0$ in (2), shaded regions in the figure]. Because all commensurable structures have been included and explicitly calculated, the ground state in the shaded regions is guaranteed to be incommensurable. Since the trial state (2) does *not* include *all possible incommensurable structures*, the true *incommensurable* ground states may be different from the ones reported here.

The structures labeled (i), (ii), and (iii) are all commensurable, i.e. the unit cell of the surface structure shown in figure 1, with a given arrangement of the eight spins, repeats itself periodically. The incommensurable structures, labeled (iv) and (v), are of two types. The stable structures in regions (iv) are the finite-amplitude "frozen" spin-waves, whose z−components are reminiscent of the bulk antiferromagnetic state, i.e. a state where the surface spins are arranged in diagonal ferromagnetic stripes with an alternating antiferromagnetic arrangement. The structure appearing in regions (v) are also "frozen" spin-waves, but their z−components are suggestive of a cross between the bulk-antiferromagnetic state and a state with the surface spins arranged in a perfect nearest-neighbor square antiferromagnet (NNSA), with the spins all pointing in the $\pm z$ direction. The subscripts a and b refer to the manner in which the second layer spins align themselves with the surface layer, i.e. generally antiparallel or parallel, respectively. Figure 3 is an example of a commensurable surface spin structure in region (ii). Figures 4, 5, and 6 are examples the incommensurable spin structures corresponding to regions (iv_a), (iv_a) and (v_a) respectively. The structures in figures 4 and 5 are, in fact, for the same values of the parameters; they have the same energy, even though their k-vectors are orthogonal to each other.

The k-vectors of the minimum-energy incommensurable states lie along either the line from Γ-to-Y or the line from Γ-to-Y′ (figure 1). By symmetry, the minimum-energy states with wavevectors $\pm$ k are degenerate. The structures in regions (iv) have an additional degeneracy: the minimum-energy state with wavevector on the line from Γ-to-Y is degenerate with the state with wavevector of the same magnitude on the line from Γ-to-Y′. This degeneracy is somewhat surprising given the domain asymmetry of the bulk configuration, but it can be easily understood[21] based on the fact that only nearest-neighbor spin interactions influence the incommensurable structure.

The value of k for the minimum energy state is very sensitive to changes in the surface exchange integrals. Extreme sensitivity occurs in the region of parameter

space near the (i)-(iii)-(iv) triple-phase-points and more generally near all the commensurable-incommensurable phase boundaries. The exchange parameters describing the surface of EuTe may be near the (i)-(iii)-(iv_b) triple-phase-point (i.e. antiferromagnetic second-nearest-neighbor exchange and ferromagnetic nearest-neighbor exchanges[3]), and hence the small changes in the nearest-neighbor surface exchange expected to arise from temperature variations could generate large, experimentally observable shifts in **k**.

A notable feature of the results presented here is that the nearest-neighbor coupling L between the surface and second layers is necessary for the stability of the incommensurable "frozen" spin waves. The surface-only nearest-neighbor exchange K, however, is not required for their stability.

IV. Conclusion

The phase-stability diagram of the simple classical Heisenberg Hamiltonian (1), found with trial states of the form (2), is remarkably complex. It shows entire regions of parameter space in which incommensurable spin structures are the stable ground state. Since *all* commensurable structures are included in this model, the incommensurable regions of the phase-stability diagram (figure 3) are certain to have incommensurable ground states, which may be the "frozen" spin waves of equation (2), or more complex *incommensurable* structures. These incommensurable surface structures are not stabilized by Fermi-surface-type effects, incommensurable or mean-field potentials, but rather are the result of competing nearest- and second-nearest-neighbor interactions. Nearest-neighbor coupling between the first and second layers seems to be necessary for the stability of the incommensurable structures.

It is possible to choose the parameters (K/J) and (L/J) to stabilize the state of any **k**-vector along the Γ-to-Y, or the Γ-to-Y$'$ line. In some regions of parameter

space, which may also coincide with the parameters corresponding to EuTe, the k-vector of the incommensurable stable state is very sensitive to small changes in (K/J) and (L/J).

Since the LEED patterns of these antiferromagnets are expected to display additional diffraction beams caused by magnetic structure at the surface, the magnetic structure factors for several interesting cases were calculated. The results, published elsewhere,[21] reveal that the LEED pattern should be very sensitive to changes in surface exchange integrals. This sensitivity, expected in both location and intensity of the diffraction beams, should be easily observed.

Acknowledgements

References

1   *New Developments in Semiconductors* , edited by P. R. Wallace, R. Harris, and M. J. Zuckermann (Noordhoff, Leyden, 1973).

2   R. Ritter, L. Jansen, and E. Lombardi, Phys. Rev. B. 8 , 2139 (1973).

3   T. Janssen, Phys. kond. Mat. 15 , 142 (1972).

4   P. W. Anderson, Phys. Rev. 115 , 2 (1959).

5   M. A. Ruderman and C. Kittel, Phys. Rev. 96 , 99 (1954).

6   B. Koiller and L. M. Falicov, J. Phys. C. 8 , 695 (1975).

7   C. Kittel, *Introduction to Solid State Physics* , 6th ed. (Wiley, New York, 1986), p. 444.

8   *Magnetic Properties of Low-dimensional Systems* , edited by L. M. Falicov and J. L. Morán-López (Springer-Verlag, Heidelberg, 1986).

9   D. Castiel, Surface Science 60 , 24 (1976).

10   V. A. Grazhulis, A. M. Ionov, and V. F. Kuleshov, Phys. Chem. Mech. Surfaces 4 , 503 (1986).

11   R. E. De Wames, Phys. Stat. Sol. 39 , 437 (1970).

12   L. M. Falicov and R. E. De Wames, Phys. Stat. Sol. 39 , 445 (1970).

13   H. C. Siegmann, Phys. Rev. 17 , 37 (1975).

14   R. H. Victora and L. M. Falicov, Phys. Rev. B. 31 , 7335 (1985).

15   L. E. Klebanoff, R. H. Victora, L. M. Falicov, and D. A. Shirley, Phys. Rev. B. 32 , 1997 (1985).

16   K. Sattler and H. C. Siegmann, Phys. Rev. Lett. 29 , 1565 (1972).

17   M. Campagna, D. T. Pierce, K. Sattler, and H. C. Siegmann, Helv. Phys. Acta. 47 , 27 (1974).

18   S. F. Alvarado, E. Kisker, and M. Campagna, in *Magnetic Properties of Low-dimensional Systems* , edited by L. M. Falicov and J. L. Morán-López (Springer-Verlag, Heidelberg, 1986) p. 52.

19   V. A. Grazhulis, private communication.

20   D. C. Chrzan and L. M. Falicov, Phys. Rev. Lett. 61 , 1509 (1988)

21   D. C. Chrzan and L. M. Falicov, Phys. Rev. B 39 , 3159 (1989)

Figure Captions

Figure 1   The unit cell and the Brillouin zone used for the calculation. All spins (indicated in stereographic projections) are in the chosen bulk configuration. The square unit cell has linear dimension b. The first label on each atom refers to each of the four simple-cubic sublattices, and the Greek label refers to each of the two face-centered-cubic sub-sublattices. The shaded atoms (labelled C and D) lie in the layer immediately below the surface, the remaining pictured spins (labelled A and B) are in the surface layer. The Γ-point corresponds to all the so-called commensurable structures. The points Y and Y′ are not equivalent because of the asymmetry of the bulk spin domain structure.

Figure 2   The phase-stability diagram for all examined structures. Regions (i), (ii), and (iii) are commensurable structures. The shaded regions are incommensurable structures. The incommensurable structures all, as found, have a single k-vector. The regions (iv) have an extra degeneracy not present in regions (v).

Figure 3   A stereographic projection of the surface spins for a structure typical of region (ii) of figure 2. The dots denote spins pointing up, and the crosses spins pointing down. The tendency toward a surface nearest-neighbor square antiferromagnet in this state is clearly evident.

Figure 4   A stereographic projection of the surface spins for a structure typical of region (iv_a). The dots denote spins pointing up, and the crosses spins pointing down. The arrow indicates the direction of k for this state. This surface state has a character similar to the bulk configuration, and is degenerate with the state pictured in figure 5.

Figure 5   A stereographic projection of the surface spins for a structure typical of region (iv_a) corresponding to the same spin parameters as used for figure

4. The dots denote spins pointing up, and the crosses spins pointing down. The arrow indicates the direction of **k** for this state. This surface state has a character similar to the bulk configuration, and is degenerate with the state pictured in figure 4.

Figure 6   A stereographic projection of the surface spins for a structure typical of region (v_a). The dots denote spins pointing up, and the crosses spins pointing down. The arrow indicates the direction of **k** for this state. A tendency towards a z-oriented nearest-neighbor square antiferromagnet is evident.

Unit Cell

Brillouin Zone
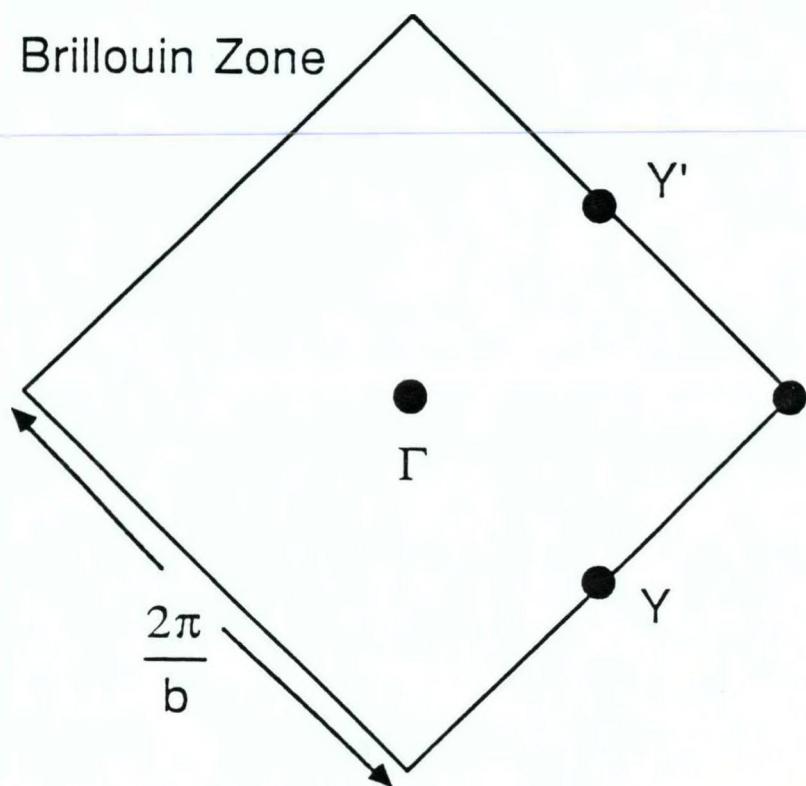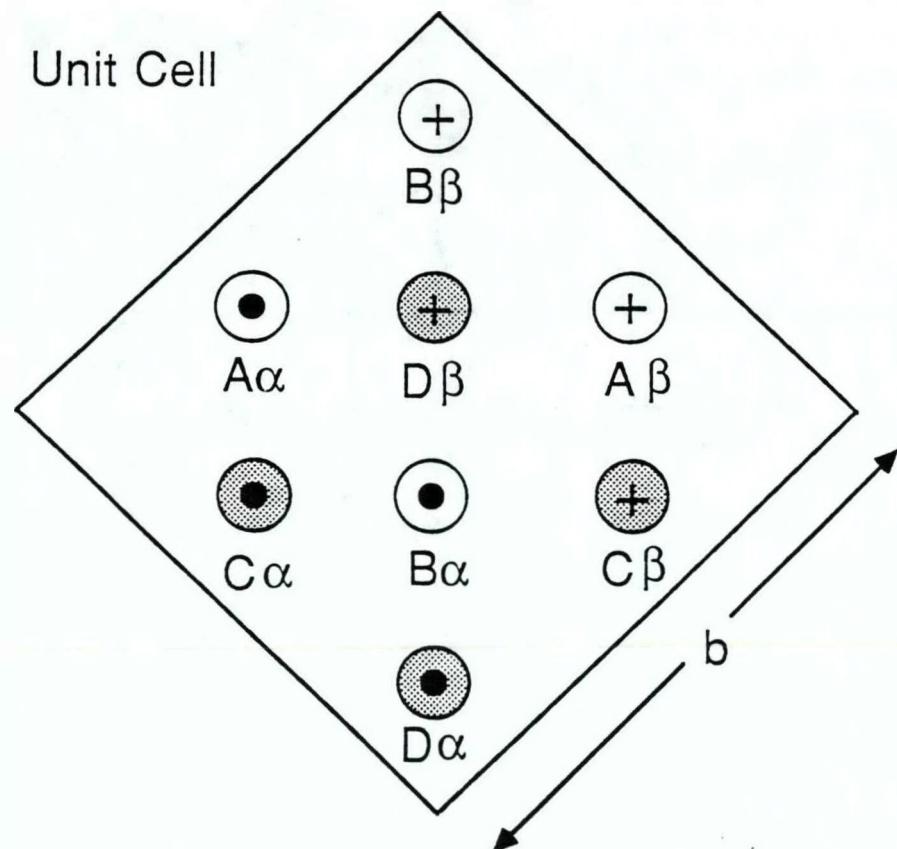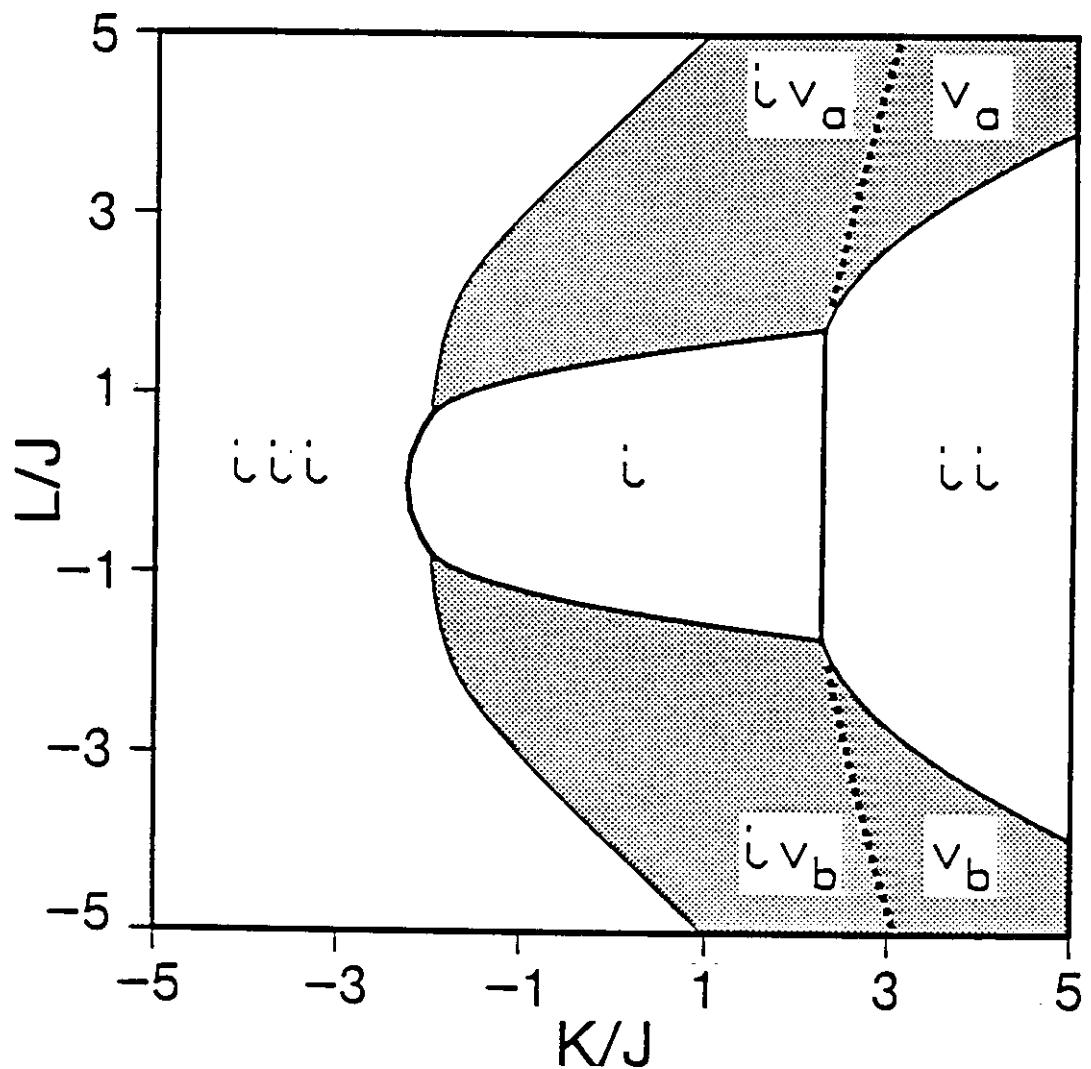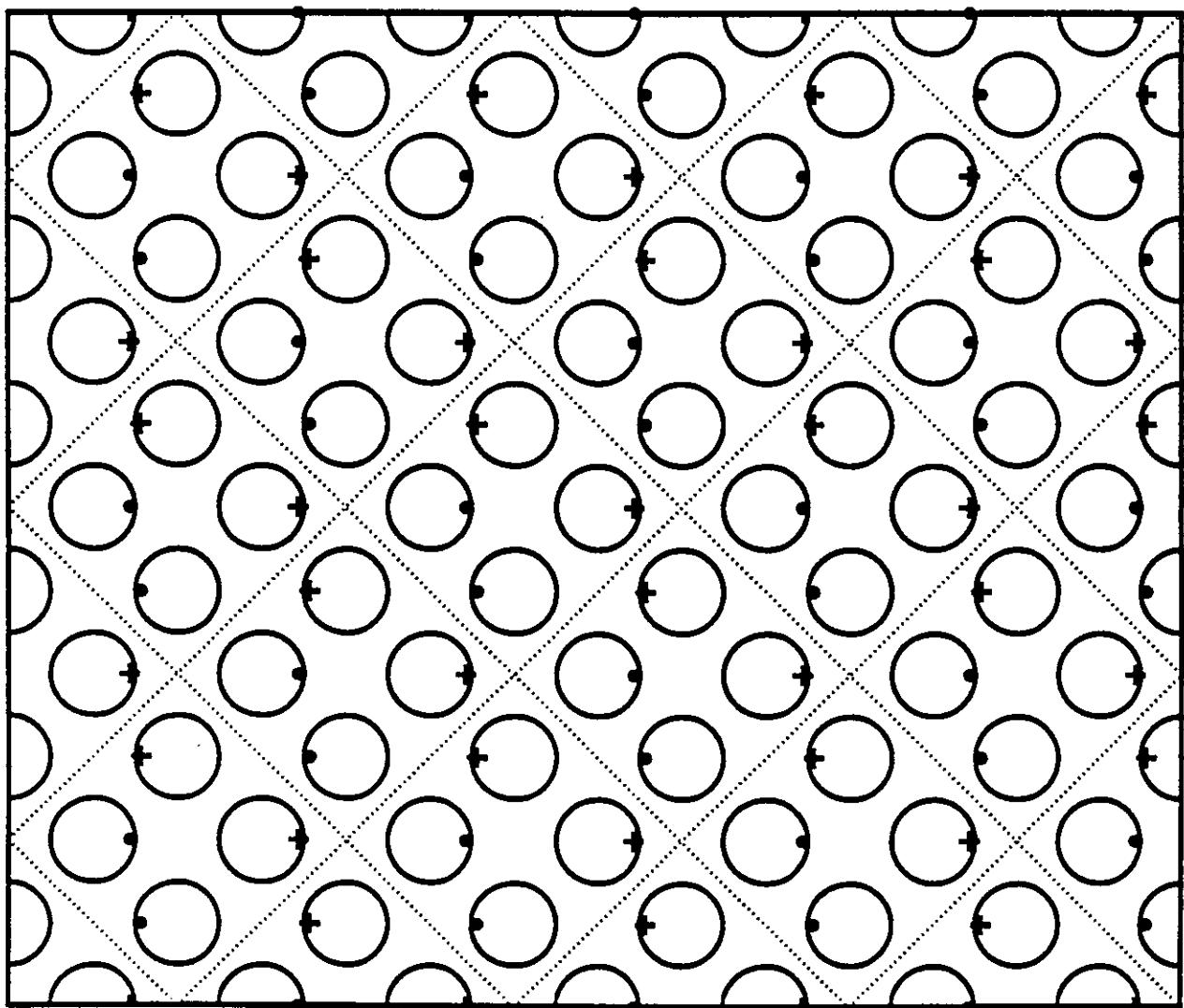
Figure   1

Figure   2

Figure   3
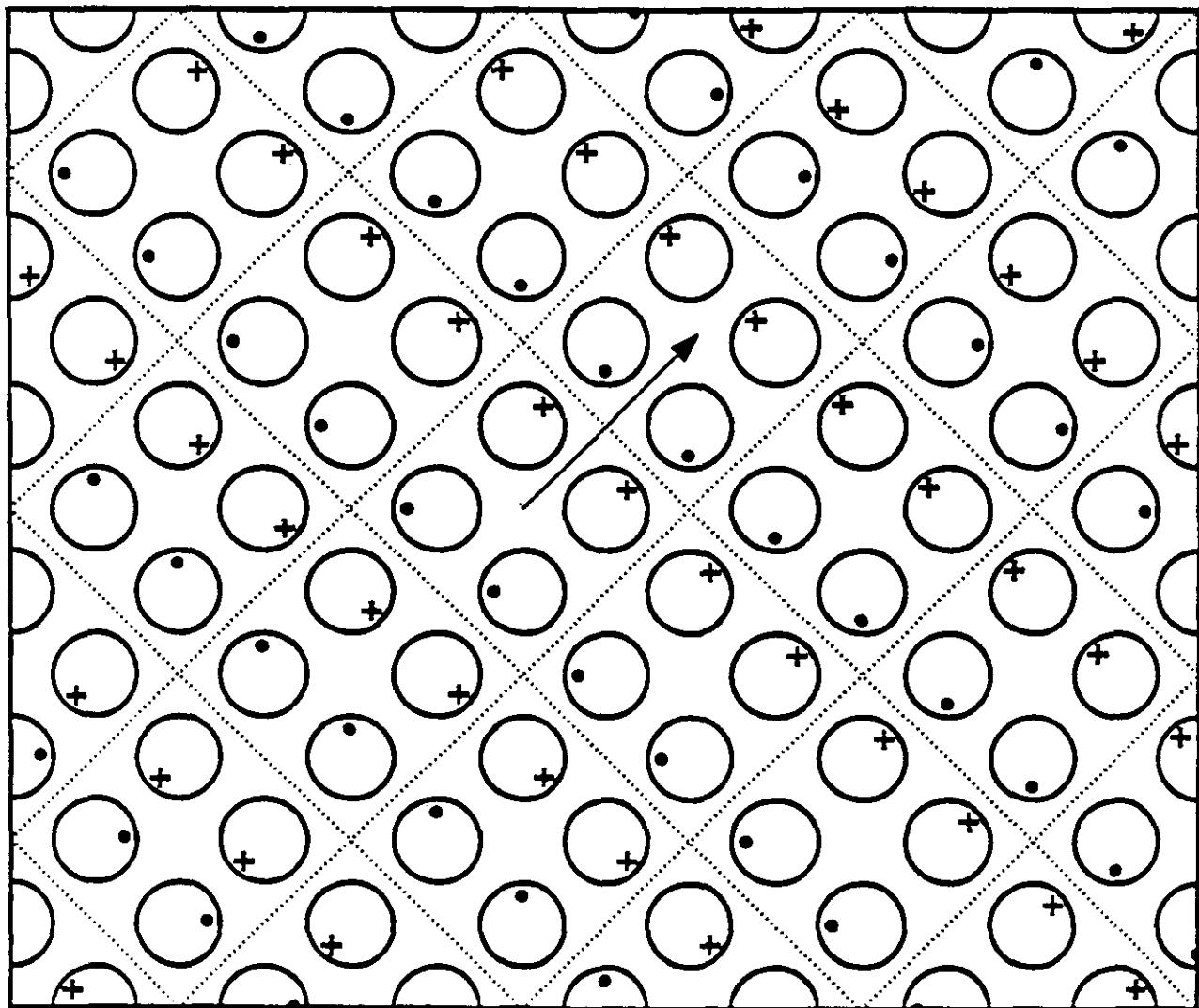
Figure   4

Figure   5

Figure   6